ARTICLE
Journal of Cellular Biochemistry 112:2424–2434 (2011)

Journal of Cellular Biochemistry

Analgesic-Antitumor Peptide Inhibits Proliferation and Migration of SHG-44 Human Malignant Glioma Cells

Youlong Zhao,[1,2] Xueting Cai,[2] Tingmei Ye,[3] Jiege Huo,[2] Chao Liu,[2] Shuangquan Zhang,[1*] and Peng Cao[2*]

[1] *Jiangsu Province Key Laboratory for Molecular and Medical Biotechnology, Life Sciences College, Nanjing Normal University, Nanjing 210097, Jiangsu, China*

[2] *Laboratory of Cellular and Molecular Biology, Jiangsu Province Institute of Traditional Chinese Medicine, Nanjing 210028, Jiangsu, China*

[3] *Department of Applied Biology, Lishui University, Lishui, 323000, Zhejiang, China*

ABSTRACT

Malignant gliomas, the most common subtype of primary brain tumors, are characterized by high proliferation, great invasion, and neurological destruction and considered to be the deadliest of human cancers. Analgesic-antitumor peptide (AGAP), one of scorpion toxic polypeptides, has been shown to have antitumor activity. Here, we show that recombinant AGAP (rAGAP) not only inhibits the proliferation of gliomas cell SHG-44 and rat glioma cell C6, but also suppresses the migration of SHG-44 cells during wound healing. To explain these phenomena, we find that rAGAP leads to cell cycle of SHG-44 arrested in G1 phase accompanied by suppressing G1 cell cycle regulatory proteins CDK2, CDK6, and p-RB by means of the down-regulated protein expression of p-AKT. Meanwhile, rAGAP significantly decreases the production of NF-κB, BCL-2, p-p38, p-c-Jun, and p-Erk1/2 and further suppresses the activation of VEGF and MMP-9 in SHG-44 cells. These findings suggest rAGAP inhibit proliferation and migration of SHG-44 cells by arresting cell cycle and interfering p-AKT, NF-κB, BCL-2, and MAPK signaling pathways. J. Cell. Biochem. 112: 2424–2434, 2011.

KEY WORDS: ANALGESIC-ANTITUMOR PEPTIDE; HUMAN ANAPLASTIC ASTROCYTOMA CELL LINE SHG-44; PROLIFERATION; CELL CYCLE; MIGRATION

Human gliomas are the most common primary brain cancers arising within the central nervous system (CNS). They are comprised of astrocytomas, oligodendrogliomas, and oligoastrocytomas and can be classified into different grades (grades I–IV) and histopathologic subgroups [Kleihues et al., 2002; Murat et al., 2008]. Especially, grade IV tumors are highly malignant, usually recalcitrant to chemotherapy, and lethal within 9–12 months [Elizabeth et al., 2001]. Gliomas are characterized by a high invasive potential and display a wide diversity of histological features. They are derived from glial support cells in the brain and the vast majority are thought to be of astrocytic origin. Malignant gliomas constitute a heterogeneous group of tumors associated with significant morbidity and mortality [Elizabeth et al., 2001]. They are aggressive, highly proliferative, greatly invasive, and neurologically destructive tumors and considered to be the deadliest of human cancers. Their abilities to invade normal brain tissue and seed new tumor growth at sites distant from the original tumor location are very impressive. Significant progress has been made in understanding pathways of glioma migration and invasion. There are several mechanisms implicated in glioma cell migration and invasion, for example, enhanced expression of matrix metalloproteinase, epidermal growth factor (EGF) receptor, and anti-apoptotic protein BCL-2, and up-regulation of several important signaling pathways such as glial cell-derived neurotropic factor [Wick et al., 1998; Woo et al., 2005; Song and Moon, 2006; Gadji et al., 2009]. In addition, it has been greatly observed in recent studies that ion channels are implicated with great importance in glioma cells. Several studies have shown that the expression of chloride, potassium, and sodium channels are up-regulated in glioma cells and these phenomena are not found in normal astrocytes [Bubien et al., 1999; Olsen et al., 2003; Warth et al., 2005]. Voltage-gated sodium channels (VGSC) are large glycoproteins composed of a major pore-forming α-subunit (250–

Grant sponsor: Natural Science Foundation of Jiangsu Province; Grant number: BK2008487; Grant sponsor: Natural Science Foundation of Zhejiang Province; Grant number: Y2090676; Grant sponsor: Jiangsu Province's Outstanding Leader Program of Traditional Chinese Medicine.

*Correspondence to: Shuangquan Zhang and Peng Cao, Laboratory of Cellular and Molecular Biology, Jiangsu Province Institute of Traditional Chinese Medicine, 100#, Shizi Street, Hongshan Road, Nanjing, Jiangsu, China. E-mail: zhangshuangquan1952@email.njnu.edu.cn, pcao79@yahoo.com

Received 17 November 2010; Accepted 21 April 2011 • DOI 10.1002/jcb.23166 • © 2011 Wiley-Liss, Inc.
Published online 2 May 2011 in Wiley Online Library (wileyonlinelibrary.com).

260 kDa) that contains the elements essential for ion conduction and voltage-dependent gating and at least two auxiliary β-subunits (30–40 kDa) that modify the channel function and participate in the targeting to the membrane [Catterall, 2000]. Now, at least 10 genes encoding α-subunits have been identified. Nine of these constitute a single family and are noted Nav1.1 to Nav1.9. In particular, the expression of Nav1.5 and Nav1.7 are related to cell migration [Mycielska et al., 2003; Diss et al., 2005; Fraser et al., 2005; Onganer and Djamgoz, 2005]. The mechanism of glioma cell migration is complex. To understand this mechanism needs more relative researches.

In traditional Chinese medicine, the scorpion *Buthus martensii* Karsch has been one of the indispensable materials used in the treatment of convulsions and epilepsy since the Sung Dynasty [Zhou et al., 1989]. Scorpion toxin contains various toxic polypeptides with different functions. Moreover, these polypeptides have been shown to affect the activities and functions of ion channels, such as sodium and potassium channels [Possani et al., 1999; Liu et al., 2002]. Analgesic-antitumor peptide (AGAP), one of these polypeptides, has been purified from the venom of *Buthus martensii* Karsch [Liu et al., 2003]. Several studies have shown that AGAP has analgesic and antitumor activities [Liu et al., 2003; Cao et al., 2010]. AGAP prolongs the survival of mice with engrafted Ehrlich ascites tumor cells greatly and suppresses the growth of S-180 fibro sarcoma efficiently [Liu et al., 2003]. Moreover, AGAP is more effective for tumor cells and less harmful for healthy cells than cyclophosphamide. Over the years, the mechanism of anti-tumor protein AGAP is still unknown. In this study, we explore and understand this mechanism.

Here, we obtained a large quantity of rAGAP with high stability and solubility as described [Cao et al., 2010]. It was found to play a role on inhibiting proliferation and migration of malignant glioma cells SHG-44, but it could not induce cell apoptosis. These results might be related to G1 cell cycle arrest and interfering some signaling pathways. In other words, AGAP down-regulated the protein expression of p-AKT and p-Erk1/2 and caused a reduction in the protein levels of CDK2, CDK6, and p-RB, finally resulting in G1 cell cycle arrest. These changes led to the inhibition of SHG-44 cells proliferation. In addition, AGAP inhibited proliferation and migration of SHG-44 cells accompanied by suppressing the protein expression of VEGF and MMP-9 by means of the down-regulation of NF-κB and BCL-2 which were regulated by the reduced activation of p-AKT, p-p38, and p-c-Jun. In summary, our results suggested rAGAP would become a promising candidate for a potential anticancer drug on patients with malignant gliomas.

MATERIALS AND METHODS

REAGENTS AND ANTIBODIES

MTT [3-(4,5-dimethylthiazol-2-yl)-2,5-diphenyltetrazolium bromide], dimethyl sulfoxide (DMSO), isopropyl β-D-1-thiogalactopyranoside (IPTG) were obtained from Sigma Chemical. DMEM medium, heat-inactivated fetal bovine serum (FBS), penicillin, and streptomycin were purchased from Gibco. Antibodies against AKT, p-AKT (ser473), BCL-2, caspase-3, caspase-8, caspase-9, cyclin E, cyclin E_2, CDK2, CDK6, cdc25A, Erk1/2, p-Erk1/2 (Thr202/Tyr204), p38, p-p38 (T182), c-Jun, p-c-Jun (T93), p-RB, VEGFA, and GAPDH were obtained from Cell Signaling Technology (Beverly, MA).

THE PREPARATION FOR RECOMBINANT AGAP

rAGAP was obtained by the expression of pET28a/SUMO-AGAP in *Escherichia coli* (*E. coli*) as described [Cao et al., 2010]. The activity of rAGAP was the same as the previous.

CELL CULTURE

Human anaplastic astrocytoma cell line SHG-44 and rat glioma cell line C6 were obtained from the Cell Bank of Chinese Academy of Sciences (Shanghai, China). The cells were maintained in DMEM (pH 7.4) supplemented with 10% FCS, 100 U/ml penicillin, 100 mg/ml streptomycin, and 0.2% $NaHCO_3$ at 37°C in a humidified atmosphere containing 95% air and 5% CO_2.

ACTIVITY AND TOXICITY ASSAYS OF rAGAP

SHG-44 and C6 Cells (1×10^4 per well) were seeded in 96-well plastic plates, respectively, and incubated at 37°C supplied with 5% CO_2 until they reached 80–90% confuency. They were treated with eight concentrations of rAGAP and incubated for 48 h. Then, 5 mg/mL MTT solution (10 μl/well) was added to each well and cells were incubated for an additional 4 h at 37°C. The supernatant was aspirated and 100 μL DMSO was added to the wells to dissolve any precipitate present. The cells were mixed with a microplate shaker for 10 min. The absorbance (A) was finally measured at an absorption wavelength of 570/630 nm by Multiskan spectrum (Thermo). All MTT assays were conducted in triplicate independent. The absorbance (A) values were presented as relative viable cell number. The growth inhibition was calculated according to the following formula: The growth inhibition ratio (IR%) = [(the absorbance of blank control group − the absorbance of experimental group)/the absorbance of blank control group] × 100%.

HOECHST 33258 STAINING ASSAY

SHG-44 cells (10×10^4 per well) were seeded in 24-well plastic plates and incubated for 24 h. Then various concentrations of rAGAP was directly added to the well and incubated for an additional 48 h. Cells were washed with PBS twice. One milliliter 4% formaldehyde was added to each well and cells were incubated for 10 min at 4°C. The supernatant was aspirated and cells were washed twice with PBS. Then, Hoechst dye solution (4 μl/well) was added to each well and cells were incubated for 10 min at room temperature in the dark. The supernatant was aspirated and cells were washed twice with PBS. Finally, 100 μl PBS was added to each well. Apoptotic cells were photographed and identified under a fluorescence microscope (Zeiss Axio Observer A1) at 340 nm.

CELL CYCLE ANALYSIS

To analyze cell cycle phase distribution, the DNA content of cells was determined by flow cytometry as described [Li et al., 2007]. After indicated treatments, cells were collected by trypsinization, washed with PBS, and fixed in ice cold 70% ethanol at 4°C overnight. After washed with PBS, cells were incubated with the DNA-binding dye propidium iodide (50 μg/ml) and RNase (1.0 mg/ml) for 30 min at 37°C in the dark. Finally, cells were washed in PBS and

flowcytometric data were acquired using a FACSCan analysis system equipped with a FACStation, MAC PowerPC computer and CellQuest Acquisition software from Becton Dickinson (FACSCalibur, Becton Dickinson). DNA histograms were analyzed using the WinMDI2.9 software. For each sample, at least 10^4 events were recorded.

MONOLAYER WOUND-HEALING ASSAY

Wound-healing assay of SHG-44 cells was performed as described previously with some modifications [Valster et al., 2005]. Briefly, before the cells were plated into this plate, two parallel lines were drawn at the underside of the well with a Sharpie marker. These lines would serve as auxiliary marks for the analyzed wound areas. SHG-44 cells were plated on a 12-well plate overnight until they reached absolute confuency. The next day, the growth medium was aspirated and two parallel scratch wounds of approximately 400 μm width were made perpendicular to the marker lines with a 200-μl sterile pipette tip, then cells were washed with PBS three times and incubated with various concentrations of rAGAP for 24 h. At last, cells were gently washed three times with PBS and photographed with an Olympus microscope (Melville, NY). The cell migration areas were quantified by Image J software. Wound closure rate was determined using the initial and final wound areas during the wounding experiments, with the percentage wound closure calculated as $[(\text{initial} - \text{final})/\text{initial}] \times 100\%$.

WESTERN BLOT

SHG-44 cells were treated with various concentrations of rAGAP (0, 10, 20, 30, and 40 μM). The treated cells were washed once with PBS, trypsinated, and centrifuged. The collected cells were washed once with PBS again, transferred to a new 1.5 ml tube and lysed on ice with lysis buffer [1% NP-40, 0.5% deoxycholate, 0.1% SDS, 68.5 mM Tris–HCl (pH 6.8), 10% glycerin] containing 1:100 protease (Sigma–Aldrich, Deisenhofen, Germany) and 1:100 phosphatase inhibitors. Protein concentrations were determined using NanoDrop1000 spectrophotometer (Thermo). The protein was denatured in boiled water for 5 min and centrifuged at 12,000 × rpm for 5 min. Equal amounts of protein were separated on 8% or 13% SDS–PAGE by electrophoresis and blotted onto PVDF membrane using the SemiPhor Semi-Dry transfer unit. Membranes were blocked for 2 h in 1% BSA (in TBST) at room temperature and then immunobloted overnight at 4°C with primary antibodies. After three washes in 0.05% Tween-20 in TBS (TBST), membranes were incubated with goat anti-mouse IgG-HRP or goat anti-rabbit IgG-HRP second antibodies (Santa Cruz) for 2 h at room temperature. Membranes were washed three times in TBST. Immunoreactive protein bands were detected with Gel/Chemi Doc System (Bio-Rad). The grayscale of the bands was detected by Adobe Photoshop CS to obtain the semi-quantitative analysis.

REVERSE TRANSCRIPTASE-POLYMERASE CHAIN REACTION (RT-PCR)

RT-PCR analysis was used to examine the mRNA expression levels of MMP-2, MMP-9, Nav1.5, and Nav1.7. RT-PCR for GAPDH was independently performed as an internal control. 1×10^7 cells were treated in the absence or presence of 10, 20, 30, and 40 μM rAGAP for 48 h. The treated cells were washed twice with PBS, trypsinated, and centrifuged. Cells were washed twice with PBS and transferred to a new tube. Total RNA was isolated from the treated cells using TRIzol reagent (Invitrogen) according to the manufacturer's protocol. The quality of RNA samples was determined by electrophoresis on agarose gel to identify the integrity of the 18S and 28S RNA bands. The concentration, purity, and amount of total RNA were determined using NanoDrop1000 spectrophotometer (Thermo). By these standards, all the RNA samples used for assay were of high quality and purity (Abs260/Abs280 > 1.7).

Total RNA (2 μg) was reversely transcribed with 200 U of M-MLV reverse transcriptase (Takara) according to standard procedures. Following inactivation of the reverse transcriptase activity, cDNA was stored at −20 °C. Oligonucleotides primers used for PCR were synthesized by Invitrogen Biological Engineering (Shanghai, China). The temperature profile included an initial denaturation for 5 min at 95°C, followed by cycle of denaturation at 95°C for 30 s, annealing at 52°C for 30 s, elongation at 72°C for 30 s. The following primers were used for identification: MMP-2 (sense: 5′-CTCCTGACATTGACCTTGGC-3′, antisense: 5′-CCTCGCTCCAGGGTGCTGGC-3′) 42 cycles, MMP-9 (sense: 5′-TTCTACGGCCACTACTGTGCC-3′, 5′-CGCCTGTGTACACCCACACC-3′) 42 cycles, Nav1.5 (sense: 5′-CACGCGTTCACTTTCCTTCG-3′, antisense: 5′-TGTGAAGAAGCTGGCTGATG-3′) 40 cycles, Nav1.7 (sense: 5′-GGCTCCTTGTTTTCTGCAAG-3′, antisense: 5′-CAGTAACATCAGCCAAGCCA-3′) 40 cycles, GAPDH (sense: 5′-CCTGACCTGCCGTCTAGAAA-3′, antisense: 5′-TTACTCCTTGGAGGCCATGT-3′) 25 cycles. The PCR products were detected by 1.0% agarose gel electrophoresis and photographed.

GELATIN ZYMOGRAPHY

The activity of MMP-2 and MMP-9, secreted in media, were detected by gelatin zymography assay as described previously [Woo et al., 2005; Jung et al., 2006]. In brief, conditioned media were concentrated by centrifugal, mixed with 2× sample buffer without a reducing agent [0.5 M Tris–HCl (pH 6.8), 10% SDS, 0.5% bromophenol blue, and 25% glycerol], and then loaded onto a 8% SDS–PAGE gel containing 0.1% (w/v) gelatin without prior boiling. After electrophoresis at 4°C, the gel was washed with washing buffer [50 mM Tris–HCl (pH 7.5), 2.5% Triton X-100 (v/v)] for 30 min at RT and the protein was allowed to renature and subsequently incubated in renaturation buffer [50 mM Tris–HCl (pH 7.5), 1 mM $ZnCl_2$, and 5 mM $CaCl_2$] at 37°C for 48 h. After the staining and destaining of the gel, the zymogram was obtained. Gelatinolytic enzymes appeared as clear bands against the blue background of the stained gel.

STATISTICAL ANALYSIS

All experiments were carried out in triplicates or duplicates and repeated at least three times. Data were processed using Microsoft EXCEL version 2003. All the results were expressed as mean ± standard deviation (SD). Statistical analyses among groups were performed using two-tailed Student's *t*-test or one-way ANOVA (SPSS13.0), the result with a P value of < 0.05 was considered statistically significant.

RESULTS

INHIBITION OF GLIOMA CELL PROLIFERATION BY rAGAP

MTT assay provides an indication of cellular proliferation and toxicity assays by way of the measure of mitochondrial dehydrogenase activity within the cell. To assess the activity of recombinant protein, we examined the effect of rAGAP on the growth inhibition of SHG-44 and C6 cells by MTT assay. Cells were incubated with eight concentrations of rAGAP for 48 h. The drug inhibited cellular proliferation in a dose-dependent manner. As shown in Figure 1, rAGAP induced a dose-dependent increase in the growth inhibition of SHG-44 and C6 cells. The percentages of growth inhibition in SHG-44 and C6 cells were from 40% to 94% at concentrations of 5, 10, 15, 20, 25, 30, 35, and 40 μM of rAGAP. After 48 h of treatment with 20 μM rAGAP, the numbers of SHG-44 and C6 living cells were reduced by 50%. From the observed results of the MTT assay, the IC50 value for SHG-44 cells and C6 cells were both 20μmol/L calculated by SPSS13.0 program.

EFFECT OF rAGAP ON GLIOMA CELL SHG-44 APOPTOSIS

Hoechst staining was used to investigate whether the treatment of rAGAP caused apoptosis. As shown in Figure 2, the Hoechst 33258 dye stained morphologically normal nuclei dimly blue. With concentration of rAGAP increased, the fluorescence intensity of the treated group with Hoechst staining was shown with strong blue fluorescence, but apoptotic bodies were not observed in significant numbers. These results showed that rAGAP did not cause cell apoptosis in SHG-44 cells.

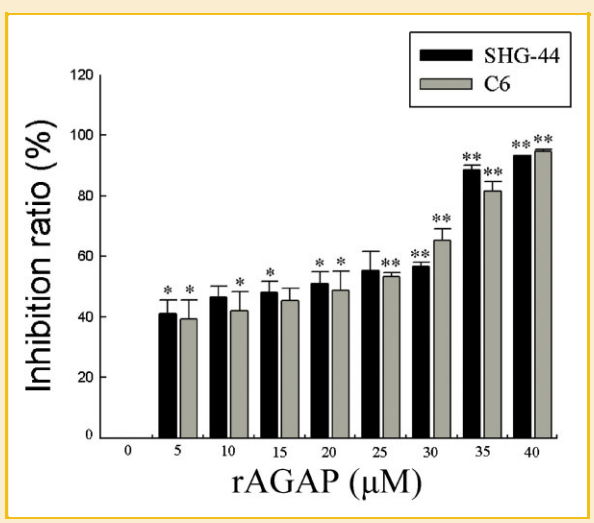

Fig. 1. Effect of rAGAP on SHG-44 and C6 cells proliferation. SHG-44 and C6 cells were treated with different concentrations of pentobarbital for 48 h. Each value was expressed as mean ± SD (n = 3). The absorbance of color produced in MTT assay was used to measure the cell proliferation. [Color figure can be seen in the online version of this article, available at http://wileyonlinelibrary.com/journal/jcb]

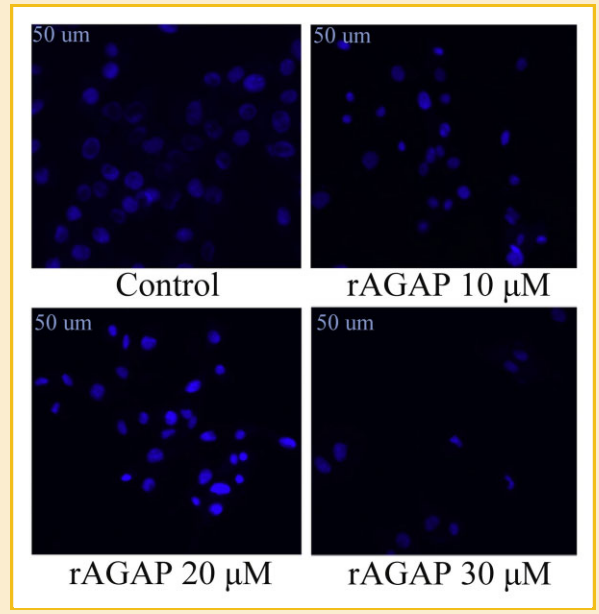

Fig. 2. SHG-44 cells were observed with a fluorescence microscope after staining with Hoechst 33258 (200× magnification). Representative figures were the SHG-44 cells treated with rAGAP at 0, 10, 20, 30 μM, respectively. Data shown here were from one of the three repeated experiments with similar results. [Color figure can be seen in the online version of this article, available at http://wileyonlinelibrary.com/journal/jcb]

EFFECTS OF rAGAP ON CELL CYCLE DISTRIBUTION OF SHG-44 CELLS

To gain insight into the mechanism of growth inhibitory effect of rAGAP, we assessed cell cycle distribution of SHG-44 cells by flow cytometry. Analysis of cell cycle showed that a dose-dependent SHG-44 accumulation in G1 phase was found to reach approximately 72.6%, 74.9%, and 78.0% of population at the concentrations of 10, 20, and 30 μM, respectively, while that in control was 64.3%, indicating cell cycle arrest at this phase. Concomitantly, there was a striking decrease in the S phase (from 20.5% of control to 9.5%, 6.7%, and 6.4% due to rAGAP treatment at 10, 20, and 30 μM). However, the percentage of cells in G2/M phase remained the same (Fig. 3A,B). These effects demonstrated cell cycle of SHG-44 cells treated by rAGAP arrested in G1 phase.

To further determine the molecular mechanism of the cell cycle G1 arrest induced by rAGAP, we examined the expression of multiple cell cycle regulatory proteins by Western blot. Two cell cycle kinases (CDK4/6-cyclin D and CDK2-cyclin E) and the transcription that included RB were pivotal in controlling the G1/S cell cycle checkpoint. Cyclin E, Cyclin E_2, CDK2, CDK6, cdc25A, and p-RB were investigated. Figure 3C showed that the expression of CDK2, CDK6, and p-RB were down-regulated with the concentrations of rAGAP increased in SHG-44 cells. Compared with the negative control, the protein expression of CDK2 merely increased by 7% at 10 μM and decreased by 25.4%, 50.1%, and 57.7% at 20, 30, and 40 μM. Moreover, the expression level of p-RB originally increased by 30% and 10% at the concentrations of 10 and 20 μM and then reduced by 35% and 54% at the concentrations of 30 and 40 μM, respectively (Fig. 3D). However, the levels of cdc25A, cyclin

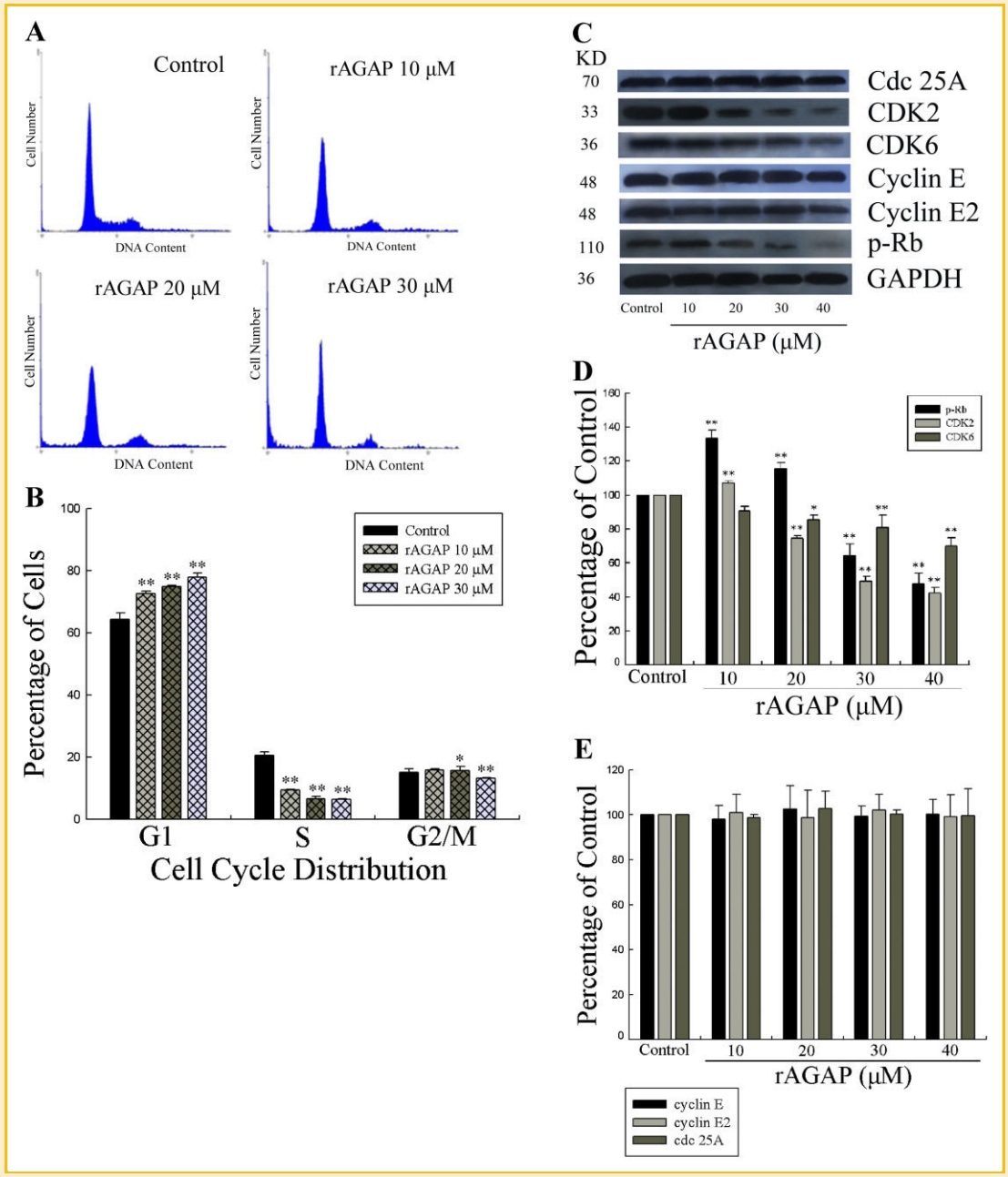

Fig. 3. Effects of rAGAP on the cell cycle and cell cycle regulatory proteins of malignant glioma SHG-44 cells. SHG-44 cells were treated with rAGAP for 48 h. A: Cell cycle distributions. One of three independent experiments was shown. B: Statistical analysis of three independent experiments, $^{*}P < 0.05$, $^{**}P < 0.01$ compared with control. C: Western blots analysis of cyclins, cyclin dependent kinases, cell division cycle 25A, and transcription complex. D,E: The quantification of band intensity was performed by densitometric analysis and presented as bar graph. The data represented the mean of three independent experiments, $^{*}P < 0.05$, $^{**}P < 0.01$ compared with control. [Color figure can be seen in the online version of this article, available at http://wileyonlinelibrary.com/journal/jcb]

E and cyclin E_2 were not altered (Fig. 3E). The inhibitory effect of rAGAP on cyclin/CDK complex expression was consistent with the reduced S phase progression. Based on these studies, rAGAP was likely to inhibit proliferation by blocking cell cycle progression through G1 to S phase by inactivation of CDK2, CDK6, and p-RB.

rAGAP SUPPRESSED SHG-44 GLIOMA CELL MIGRATION

Apart from the infinite proliferation ability, migration, and invasion are another characteristic feature of malignant gliomas. To evaluate the possibilities for limiting glioma cell migration by inhibition of rAGAP, we performed a scratch-migration-assay. When comparing four different rAGAP concentrations, there was an apparent phenomenon that untreated SHG-44 cells were able to invade the scratched area which was recolonized in the majority 24 h later (Fig. 4). However, rAGAP strongly impaired this process in a dose-dependent fashion. In fact, only a small minority of cells in 30 μM rAGAP group was in the scratched area 24 h later and the distance between the borders of the wound was significantly different from

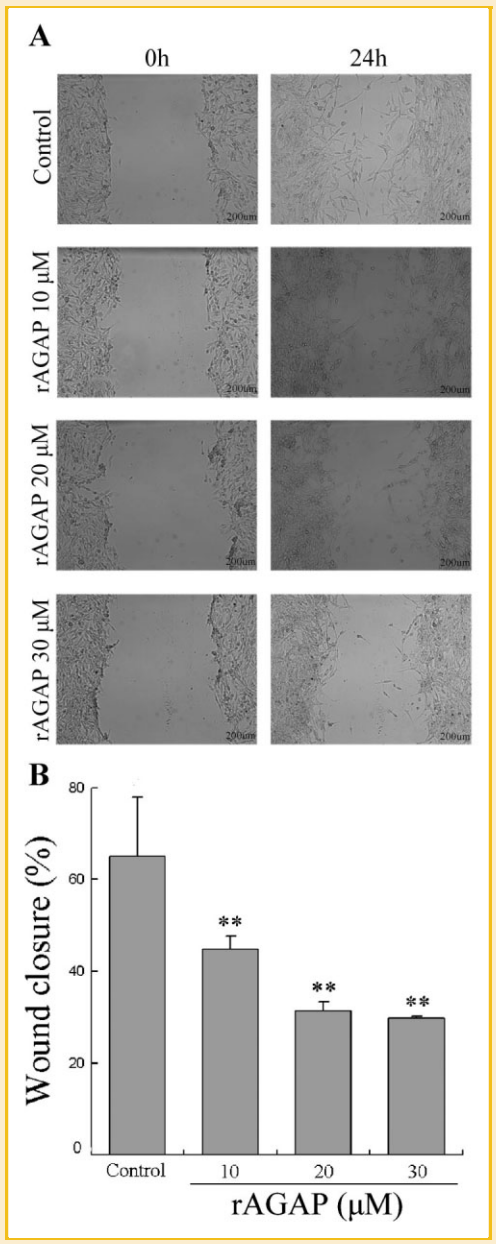

Fig. 4. rAGAP inhibited the migration of SHG-44 cells in vitro. SHG-44 cells (2×10^5 cells/well; 12-well plates) were scraped with a 200-μl sterile pipette tip and treated with 0, 10, 20, and 30 μM rAGAP for 24 h. Cells were photographed under phase-contrast microscopy (100× magnification). A: The contrast of cell migration area between 0 and 24 h was observed under the microscope. Representatives of three independent experiments are shown. B: The quantification of cell migration areas was performed and presented as bar graph. The data represented the mean of three independent experiments, $^{*}P < 0.05$, $^{**}P < 0.01$ compared with control.

that of the control after the scratch (Fig. 4). Quantitative analysis clearly indicated significant decreases ($P < 0.05$) of the cell migration rate with rAGAP at concentrations of 10, 20, and 30 μM for 24 h in wound closure compared to the control. These data suggested that rAGAP have the ability to suppress the migration of SHG-44 cells.

EXPRESSION OF PROLIFERATION, MIGRATION, AND APOPTOSIS-RELATED PROTEINS BY rAGAP TREATMENT

To further explore the inhibition of SHG-44 cellular migration involved in some signal pathways, the expression levels of various intracellular proteins in a dose-dependent change were evaluated. The cells were treated with rAGAP. We firstly measured the total protein levels of caspase-3, -8, and -9 to further confirm the statement that rAGAP brought SHG-44 cells to apoptosis. Western blotting of inactive caspase precursor did not reveal a significant change and the active cleaved-caspase 3, 8, 9 were not observed (Fig. 5). These results indicated that the precursors of these proteins were not cleaved into the fragment and not activated. This further demonstrated that rAGAP did not cause cell apoptosis in SHG-44 cells. As shown in Figure 5, anti-apoptotic protein BCL-2 and nuclear factor NF-κB/p65 were significantly down-regulated in a dose-dependent manner. In addition, the protein levels of p-AKT, p-p38, p-Erk1/2, p-c-Jun, and VEGF were gradually decreased with the increase of rAGAP concentrations. However, the levels of MMP-2 in cell and medium were not altered and the total protein level of BAX was not detectable (data not shown). These results demonstrated that rAGAP might inhibit SHG-44 cells proliferation and migration through BCL-2, NF-κB/p65, AKT, and MAPK signaling pathway, whereas the apoptotic signaling pathways was not involved in.

EXPRESSION OF PROLIFERATION AND MIGRATION-RELATED GENES BY rAGAP

The mechanism that rAGAP inhibited SHG-44 cells proliferation and migration was complex, so we studied some genes changes in the mRNA levels. The down-regulation of Nav1.5 and MMP-9 was seen in SHG-44 cells treated by rAGAP in a dose-dependent manner. However, the total mRNA levels of Nav1.7 and MMP-2 were detected without changes (Fig. 6). These studies showed that rAGAP might suppress proliferation and migration of SHG-44 cells by way of the mRNA expression of Nav1.5 and MMP-9 in a dose-dependent change.

ZYMOGRAPHY ANALYSIS

Gelatinases, such as MMP-2 and MMP-9, have been shown to be elevated in glioma tissue samples and play a major role in glioma invasion and migration [Kim et al., 2005; Woo et al., 2005]. In this study, we detected gene and protein expression of these two MMPs in SHG-44 cells treated by several concentrations of rAGAP. In the negative control, cultured SHG-44 constitutively expressed MMP-9 protein. However, in the treated group, the expression of MMP-9 was gradually down-regulated at the protein level with the concentrations of rAGAP increased (Fig. 7), but the expression of MMP-2 was shown without change (result not shown). The truth showed that rAGAP might suppress SHG-44 cells migration by reducing the protein expression of MMP-9.

DISCUSSION

Malignant gliomas are the most common subtype of primary brain tumors within the CNS. Among various histological types of CNS

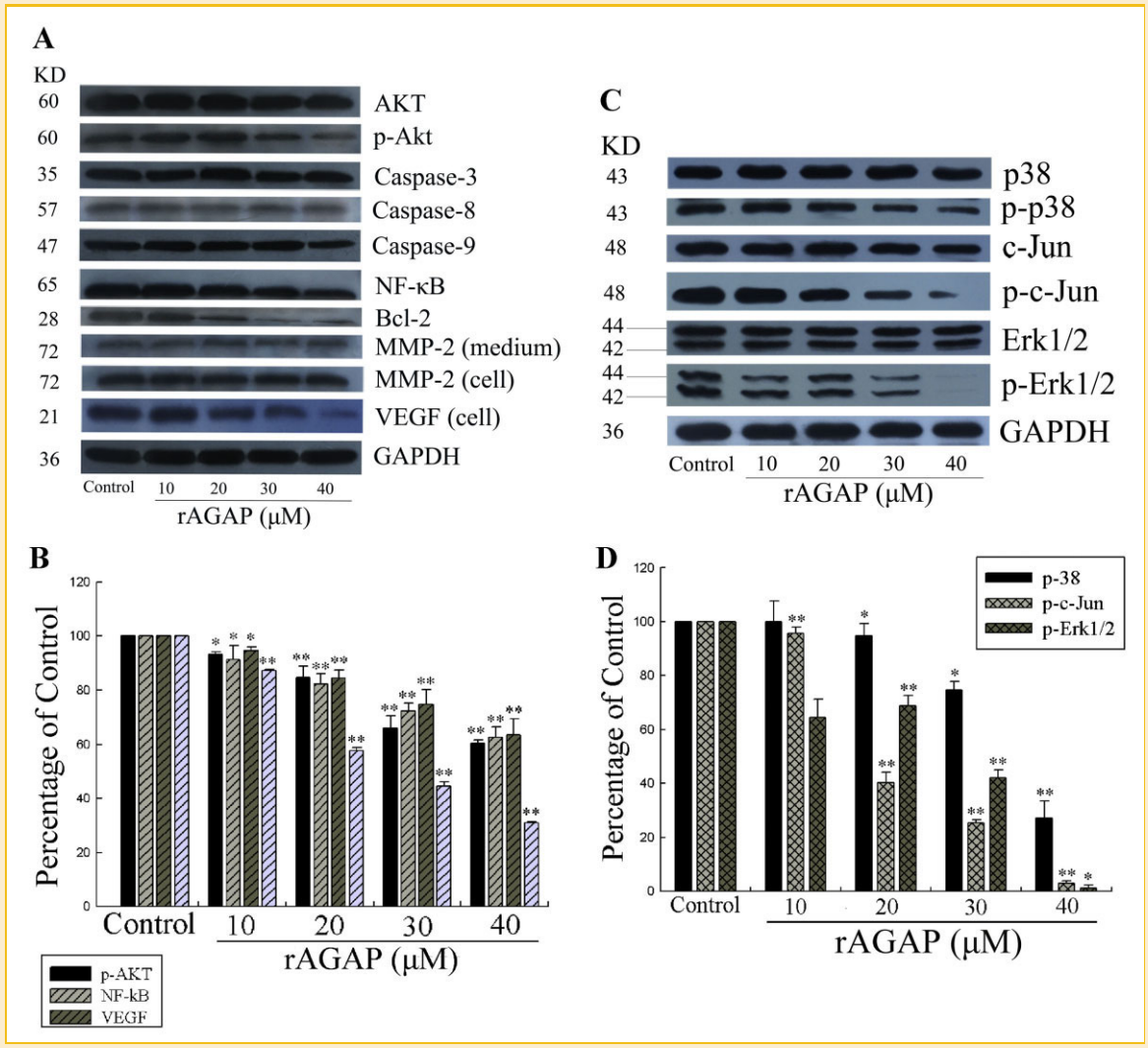

Fig. 5. Representative Western blot showed the changes in the levels of associated proteins in cell proliferation and migration of SHG-44 cells treated with rAGAP. The SHG-44 cells (5×10^6 cells/well) were treated with rAGAP at 0, 10, 20, and 30 μM, then the total protein was prepared and determined, as described in Materials and methods. A,C: The expression levels of AKT, p-AKT, p38, p-P38, Erk1/2, p-Erk1/2, Jun, p-c-Jun, BCL-2, caspase-3, caspase-8, caspase-9, MMP-2 (cells or cell culture medium), NF-κB/p65, VEGF (cells) and GAPDH were estimated by Western blot, as described in Materials and Methods section. B, D, and E: The quantification of band intensity was performed by densitometric analysis and presented as bar graph. The data represented the mean of three independent experiments, $^{*}P < 0.05$, $^{**}P < 0.01$ compared with control. [Color figure can be seen in the online version of this article, available at http://wileyonlinelibrary.com/journal/jcb]

glioma, malignant tumor from astrocytic origin is characterized by their aggressiveness, high invasiveness, and great neovascularization. In addition, neurologically destructive tumors are considered to be the deadliest of human cancers [Bian et al., 2004]. Although various treatments for gliomas are developing, the expectancy of patients with malignant glioma is poor. To explore the pathogenic mechanism and find a better understanding of glioma biology are essential for deriving more effective therapeutics for such an incurable CNS neoplasm [Maher et al., 2001].

In traditional Chinese medicine, the scorpion *Buthus martensii* Karsch has been one of the indispensable materials used in the treatment of many diseases such as convulsions and epilepsy since the Sung Dynasty [Zhou et al., 1989; Tan and Guo, 2006]. Scorpion toxin contains various toxic peptides with different functions and these peptides have been shown to affect the activities and function of ion channels, such as sodium channels [Possani et al., 1999]. AGAP is one of these toxin peptides. Sequence comparison at the amino acid level demonstrates that AGAP shows the high homology with nine kinds of scorpion toxin, such as alpha-toxin-4, alpha-toxin-beml, bukatoxin, neurotoxin-tx15, sodium-bukta, toxin-bmka1, toxin-bmkt, toxin-buktta3, and toxin-bmktatx15. In particular, it shares 86.36% similarity to bukatoxin (result not shown). Moreover, nine kinds of scorpion toxin are Na^+-channel specific inhibitor. AGAP consists of 66 amino acid residues and is one of scorpion alpha-toxins which belong to Na^+-channel specific scorpion toxins. Together, AGAP may be the inhibitor of sodium channel toxin. In addition, the above study has shown that the mRNA level of Nav1.5 was down-regulated in SHG-44 cells treated by AGAP in a dose-dependent manner. It further allows for the statement that AGAP might be a Na^+-channel-specific inhibitor.

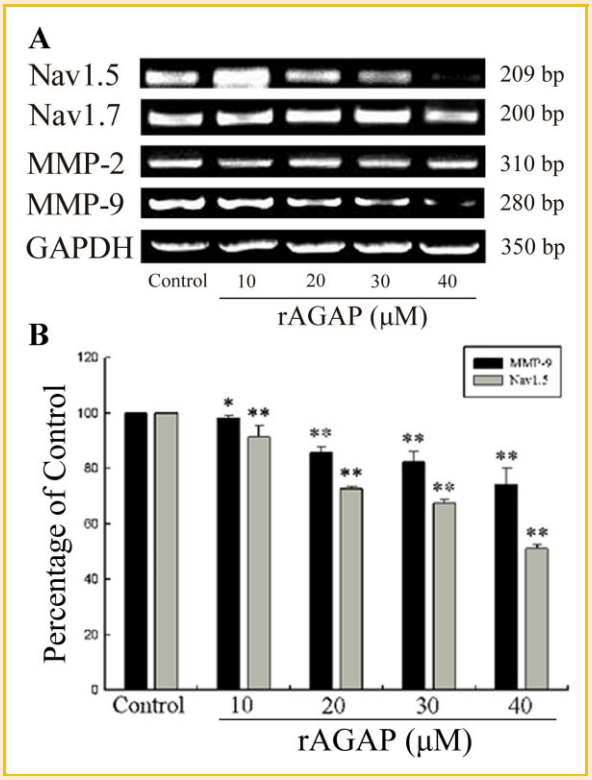

Fig. 6. Effect of rAGAP on gene expression of GAPDH, Nav1.5, Nav1.7, MMP-2, and MMP-9 in cultured SHG-44 cells. Cells were treated with rAGAP at 0, 10, 20 30, and 40 μM for 48 h. A: RT-PCR analysis of mRNA expression. B: Semi-quantified using image analysis, $^{*}P < 0.05$, $^{**}P < 0.01$ compared with control. [Color figure can be seen in the online version of this article, available at http://wileyonlinelibrary.com/journal/jcb]

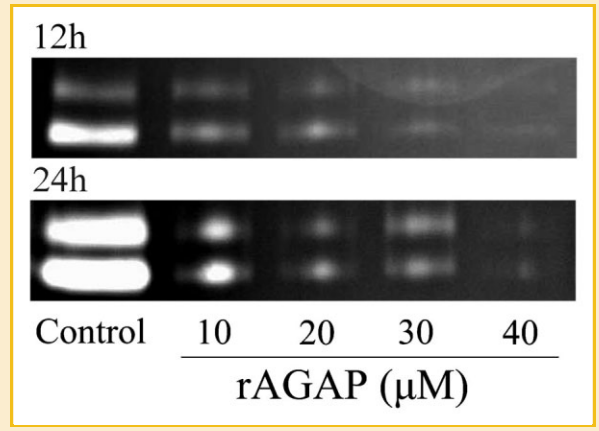

Fig. 7. Gelatin zymography of MMP-9. The bands indicate MMP-9 activity. A: MMP-9 collected from the culture medium of SHG-44 cells cultured with rAGAP at 0, 10, 20 30, and 40 μM for 12 h. B: MMP-9 collected from the culture medium of the same number of SHG-44 cells cultured with rAGAP at 0, 10, 20 30, and 40 μM for 24 h.

rAGAP has been purified from the venom of *Buthus martensii* Karsch [Liu et al., 2003; Cao et al., 2010]. Several studies have shown that rAGAP has analgesic and antitumor activities. It can inhibit the proliferation and growth of tumor cells, but the mechanisms of these phenomena are unknown. The main reason is that these scorpion toxins are ion channel inhibitor and the complexity of structures and function involved in ion channel have not been absolutely mastered. In the current study, the statement that rAGAP brought SHG-44 cells to apoptosis was not sure, because apoptotic bodies were not observed in significant numbers. In addition, the experiments of DNA ladder that rAGAP induced SHG-44 cells in a dose- and time-dependent manner showed that DNA ladder did not occurred (result not shown). This allowed for the above statement. Apart from these, we detected the protein expression of the caspases essential in cells for apoptosis. Caspase-3, -8, and -9 were extremely important in the apoptosis signaling pathway. The expression levels of their total typical apoptotic proteins were seen without changes and the cleaved fragment of them was not observed. This event further supported the above statement. In summary, rAGAP did not cause SHG-44 cell apoptosis.

Blockage of cell cycle progression is an important reason that leads to inhibit the proliferation of tumor cells. The G1/S-phase checkpoint, the first critical restriction point in the cell division cycle, controls the passage of eukaryotic cells from the first "gap" phase (G1) into the DNA synthesis phase (S). The G1/S transition is closely linked to the activation of cell cycle kinases such as cyclins, CDKs, and the transcription complex that includes RB [Nurse, 2000]. In our study, the data of flow cytometry showed that cell cycle induced by rAGAP in SHG-44 cell arrested in G1 phase, accompanied by the reduction in S phase and no change in G2/M phase. To understand the mechanism about SHG-44 cell arrested in G1 phase, the expression of cell cycle protein was detected by Western blot. The expression of CDK2, CDK6, and p-RB were down-regulated in a dose-dependent manner. As was well known, the cell cycle from G1 to S phase was regulated by cyclin D/CDK4 (CDK6) or cyclin E/CDK2 complexes. Cyclin/CDK complexes mediated RB phosphorylation in late G1 phase, and hyperphosphorylated RB induced the release of the transcription factor E2F, resulting in cell cycle progression to S phase. In our result, the expression levels of CDK2 and p-RB were increased at low concentrations (10–20 μM) of rAGAP and decreased at high concentrations (30–40 μM) of rAGAP compared with the negative control. The reason that this phenomenon occurred might be that rAGAP affected the Na^{+} current or Na^{+} influx by inhibiting the Nav1.5 mRNA expression, contributed to altering electrophysiological properties of cancer cells, causing the perturbation of their intracellular ionic homeostasis or resulting in energy shortages. As was well known, DNA synthesis was related to Na^{+}. Thus, rAGAP might interfere with DNA synthesis directly and partially and result in the death of few SHG-44 cells. The accumulation of CDK2 in dead cell contributed to increasing the total amount of CDK2 and p-RB. However, when high concentrations of rAGAP-treated SHG-44 cells, they decreased the expression of CDK2 and CDK6 and caused the activation of p-RB a sharp reduction, finally resulting in cell cycle arrest in G1 phase. In addition, the protein expression of p-AKT, a cytoplasmic serine/threonine protein kinase, was decreased. Inhibiting the activity of AKT kinase brought about a decline in the expression of CDK2 [Shin et al., 2002]. In conclusion, these results involved in cell cycle

confirmed the pathway that the down-regulation expression of p-AKT leaded to a decline in the expression of CDK2 and CDK6, finally resulting in a reduction in the protein of p-RB. This pathway might contribute to the cell cycle arrest in G1 phase and inhibiting the proliferation of SHG-44 cells.

The infiltration of malignant gliomas cells and their high proliferative activity are key elements in turning the local adjacent tissue to tumor lesion. More important, cell migration is a crucial event for tumor spreading, metastasis, and invasiveness. Recently, ion channels are gradually and increasingly being proved to be involved in different aspects/stages of the cancer process, including proliferation [Fraser et al., 2002] and migration [Diss et al., 2004]. Especially, the expression of VGSCs has been shown to be up-regulated in several human cancers (in vitro and in vivo), including breast cancer [Fraser et al., 2005], prostate cancer [Diss et al., 2005], and small-cell lung cancer [Onganer and Djamgoz, 2005]. The up-regulation of functional VGSCs is viewed as the reason for metastatic cell behavior such as motility, adhesion, invasion, and endocytosis [Mycielska et al., 2003; Diss et al., 2005; Fraser et al., 2005; Onganer and Djamgoz, 2005]. The inhibition of the Na+ current they carry decreases glioma growth and cell migration [Vila-Carriles et al., 2006; Kapoor et al., 2009]. Moreover, augmented Na^+ influx due to the overexpression of Na^+ permeable voltage-gated (Nav1.5 and Nav1.7) [Prevarskaya et al., 2010]. In a word, cell migration is closely linked with VGSCs. In the current study, the mRNA expression of Nav1.5 voltage-gated Na^+ channel was down-regulated in dose-dependent manner, whereas there was no change in the total mRNA expression of Nav.1.7 voltage-gated Na^+ channel. These results showed that rAGAP inhibited the Nav1.5 mRNA expression and further suppressed the migration of SHG-44 cells.

Using a wound-healing assay in vitro, which was involved in both cell proliferation and migration, we found that SHG-44 cell wound closure exhibited a bell-shape curve in response to different dose of rAGAP, suggesting that the migration of SHG-44 cell mainly led to wound closure. This demonstrated that rAGAP inhibited the migration of SHG-44 cells. To explain this phenomenon, the protein expression was detected by Western blot and zymography analysis. These results showed that the expression levels of p-AKT, NF-κB, BCL-2, p-p38, p-Erk1/2, p-c-Jun, VEGF, and MMP-9 were down-regulated. The activation of serine/threonine kinase Akt was linked to the enhancement of NF-κB nuclear localization and transactivation [Dhawan et al., 2002]. It was well known that p-AKT regulated BCL-2 by PI3K-Akt-BCL-2 signaling pathway. Therefore, when rAGAP-treated SHG-44 cells in dose-dependent manner, the expression levels of NF-κB and BCL-2 were gradually down-regulated with the activation of p-AKT suppressed. The down-regulation of NF-κB and BCL-2 did not induce SHG-44 cell apoptosis. There was a possible reason that rAGAP affected the Na^+ current or Na^+ influx by inhibiting the Nav1.5 mRNA expression, resulted in blocking DNA synthesis, the perturbation of their intracellular ionic homeostasis or energy shortages. These might contributed directly to the death of SHG-44 cells without the apoptotic process. In addition, Erk1/2 (extracellular signal-regulated kinase), JNK/SAPK (C-Jun N-terminal kinase/stress-activated protein kinase) and p38 kinase belonged to MAPK families of serine/threonine protein kinases. Erk1/2 activation-induced cell proliferation and activation of p38 promoted cell migration [Sharma et al., 2003]. Both p38 and Erk1/2 were translocated to the nucleus and further phosphorylate-specific transcription factors to regulate gene expression. Erk1/2 regulated MMP-9 by way of NF-κB signaling pathway [Moon et al., 2004]. The JNK pathway regulated NF-κB-mediated gene transcription through its phosphorylation and activation of c-Jun [Tuyt et al., 1999]. rAGAP could inhibit proliferation of SHG-44 cells by means of suppressing the activation of p-Erk1/2 and migration of SHG-44 cells involved in decreasing the protein expression of p-AKT, p-p38, and p-c-Jun.

NF-κB, a key regulator of immune and inflammatory response, could regulate the processes of cell growth, migration, and invasion. Several studies had shown the suppression of cell tumor angiogenesis and metastasis partly through the inhibition of NF-κB and its target genes MMPs and VEGF, and inhibition of NF-κB-reduced expression of MMP-9 and VEGF and activity of the MMP-9 promoter reporter [Fujioka et al., 2003; Ogawa et al., 2004; Schmidt et al., 2007]. In addition, anti-apoptotic protein BCL-2 promoted migration and invasiveness of human glioma cells by increasing the expression of matrix metalloproteinase such as MMP-9 [Wick et al., 1998]. Gelatinases, such as MMP-9, played a major role in glioma invasion and migration [Kim et al., 2005; Woo et al., 2005]. VEGF, one of the most potent angiogenic factors, increased glioma cell proliferation and invasion [Hong et al., 2006]. Taken together, with the concentration of rAGAP increased, the protein levels of NF-κB and BCL-2 in treated SHG-44 cells were gradually down-regulated by means of suppressing the protein expression of p-AKT, p-Erk1/2, p-c-Jun, and p-p38 in dose-dependent manner. Meanwhile, there was a corresponding reduction in the total amounts of VEGF and MMP-9 by the regulation of NF-κB and BCL-2. rAGAP finally inhibited proliferation of SHG-44 cells by means of suppressing the activation of p-Erk1/2 and migration of SHG-44 cells in a wound-healing assay involved in targeting Erk, p38, c-Jun MAPK, and AKT pathway.

In conclusion, we found here that rAGAP might be the inhibitor of Nav1.5 and perturbed intracellular ionic homeostasis by inhibiting the expression and activity of Nav1.5 in SHG-44 cells, resulting in down-regulation of the protein activation of p-AKT, p-p-38, p-Erk1/2, and p-c-Jun. These changes triggered some signaling cascades. On the one hand, decreasing p-AKT expression down-regulated the protein levels of CDK2 and CDK6 and further reduced activation of p-RB, finally leading to cell cycle arrest in G1 phase. On the other hand, the protein expression of NF-κB and BCL-2 was gradually reduced by suppressed activation of p-AKT, p-p-38, p-Erk1/2, and p-c-Jun, respectively, finally decreasing the protein levels of VEGF and MMP-9. These events eventually inhibited proliferation and migration of malignant glioma SHG-44 cells.

We have demonstrated that rAGAP suppresses proliferation and migration of SHG-44 cells by cell cycle arrest in G1 phase and blocking some signaling pathway such as AKT, Erk, p38, c-Jun MAPK, NF-κB, and BCL-2. As an active polypeptide of scorpion toxin, rAGAP may prove to be a novel candidate for treating the multimodality of malignant gliomas. There will be more hope of a cure for cancer patients with malignant gliomas.

ACKNOWLEDGMENTS

This work was supported by Jiangsu Province's Outstanding Leader Program of Traditional Chinese Medicine, Natural Science Foundation of Jiangsu Province (No. BK2008487) and Natural Science Foundation of Zhejiang Province (No. Y2090676).

REFERENCES

Bian XW, Chen JH, Jiang XF, Bai JS, Zhang X. 2004. Angiogenesis as an immunopharmacologic target in inflammation and cancer. Immunopharmacology 4:1537–1547.

Bubien JK, Keeton DA, Fuller CM, Gillespie GY, Reddy AT, Mapstone TB, Benos DJ. 1999. Malignant human gliomas express an amiloridesensitive Na^+ conductance. Am J Physiol Cell Physiol 276:C1405–C1410.

Cao P, Yu JM, Lu WG, Cai XT, Wang ZG, Gu ZH, Zhang J, Ye TM, Wang M. 2010. Expression and purification of an antitumor-analgesic peptide from the venom of Meso*buthus martensii* Karsch by small ubiquitin-related modifier fusion in *Escherichia coli*. Biotechnol Prog 26:1240–1244.

Catterall WA. 2000. From ionic currents to molecular mechanisms: The structure and function of voltage-gated sodium channels. Neuron 26:13–25.

Dhawan P, Singh AB, Ellis DL, Richmond A. 2002. Constitutive activation of Akt/protein kinase B in melanoma leads to up-regulation of nuclear factor-κB and tumor progression. Cancer Res 62:7335–7342.

Diss JKJ, Fraser SP, Djamgoz MBA. 2004. Voltage-gated Na^+ channels: Multiplicity of expression, plasticity, functional implications and pathophysiological aspects. Eur Biophys J 33:180–193.

Diss JKJ, Stewart D, Pani F, Foster CS, Walker MM, Patel A, Djamgoz MBA. 2005. A potential novel marker for human prostate cancer: Voltage-gated sodium channel expression in vivo. Prostate Cancer Prostatic Dis 8:266–273.

Elizabeth A, Maher FB, Furnari RM, Bachoo. 2001. Malignant glioma: genetics and biology of a grave matter. Genes Dev 15:1311–1333.

Fraser SP, Koyuturk M, Djamgoz MBA. 2002. Ion channel activity and cancer cell proliferation:Ashort review with particular reference to prostate cancer. In: Rouzaire-Dubois IB, Benoit E, Dubois JM, editors. Ion channels and physiopathologies of nerve conduction and cell proliferation. Kerala, India: Research Signpost. pp. 153–172.

Fraser SP, Diss JKJ, Chioni AM, Mycielska ME, Pan H, Yamaci RF, Pani F, Siwy Z, Krasowska M, Grzywna Z, Brackenbury WJ, Theodorou D, Koyutürk M, Kaya H, Battaloglu E, Bella MTD, Slade MJ, Tolhurst R, Palmieri C, Jiang J, Latchman DS, Coombes RC, Djamgoz MBA. 2005. Voltage-gated sodium channel expression and potentiation of human breast cancer metastasis. Clin Cancer Res 11:5381–5389.

Fujioka S, Sclabas GM, Schmidt C, Niu JG, Frederick WA, Dong QG, Abbruzzese JL, Evans DB, Baker C, Chiao PJ. 2003. Inhibition of constitutive NF-κB activity by IκBαM suppresses tumorigenesis. Oncogene 22:1365–1370.

Gadji M, Crous AT, Fortin D, Krcek J, Torchia M, Mai S, Drouin R, Klonisch T. 2009. EGF receptor inhibitors in the treatment of glioblastoma multiform: Old clinical allies and newly emerging therapeutic concepts. Eur J Pharmacol 625:23–30.

Hong X, Jiang F, Kalkanis SN, Zhang ZG, Zhang XP, DeCarvalho AC, Katakowski M, Bobbitt K, Mikkelsen T, Chopp M. 2006. SDF-1 and CXCR4 are up-regulated by VEGF and contribute to glioma cell invasion. Cancer Lett 236:39–45.

Jung SH, Woo MS, Kim SY, Kim WK, Hyun JW, Kim EJ, Kim DH, Kim HS. 2006. Ginseng saponin metabolite suppresses phorbol ester-induced matrix metalloproteinase-9 expression through inhibition of activator protein-1 and mitogen-activated protein kinase signaling pathways in human astroglioma cells. Int J Cancer 118:490–497.

Kapoor N, Bartoszewski R, Qadri YJ, Bebok Z, Bubien JK, Fuller CM, Benos DJ. 2009. Knockdown of ASIC1 and epithelial sodium channel subunits inhibits glioblastoma whole cell current and cell migration. J Biol Chem 284:24526–24541.

Kim SY, Jung SH, Kim HS. 2005. Curcumin is a potent broad spectrum inhibitor of matrix metalloproteinase gene expression in human astroglioma cells. Biochem Biophys Res Commun 337:510–516.

Kleihues P, Louis DN, Scheithauer BW, Rorke LB, Reifenberger G, Burger PC, Cavenee WK. 2002. The WHO classification of tumors of the nervous system. J Neuropathol Exp Neurol 61:215–225.

Li Y, Yin W, Wang X, Zhu W, Huang Y, Yan G. 2007. Cholera toxin induces malignant glioma cell differentiation via the PKA/CREB pathway. Proc Natl Acad Sci USA 104:13438–13443.

Liu YF, Hu J, Zhang JH, Wang SL, Wu CF. 2002. Isolation purification and N-terminal partial sequence of an antitumoral peptide from the venom of the Chinese scorpion *Buthus martensii* Karsch. J Prepar Biochem Biotechnol 32:317–327.

Liu YF, Ma RL, Wang SL, Duan ZY, Zhang JH, Wu LJ, Wu CF. 2003. Expression of an antitumor-analgesic peptide from the venom of Chinese scorpion *Buthus martensii* Karsch in *Escherichia coli*. J Protein Expr Purif 27:253–258.

Maher EA, Furnari FB, Bachoo RM, Rowitch DH, Louis DN, Cavenee WK, DePinho RA. 2001. Malignant glioma: Genetics and biology of a grave matter. Genes Dev 15:1311–1333.

Moon SK, Cha BY, Kim CH. 2004. ERK1/2 mediates TNF-α-induced matrix metalloproteinase-9 expression in human vascular smooth muscle cells via the regulation of NF-κB and AP-1: Involvement of the ras dependent pathway. J Cell Physiol 198(3): 417–427.

Murat A, Migliavacca E, Gorlia T, Lambiv WL, Shay T, Hamou MF, Tribolet N, Regli L, Wick W, Kouwenhoven MC, Hainfellner JA, Heppner FL, Dietrich PY, Zimmer Y, Cairncross JG, Janzer RC, Domany E, Delorenzi M, Stupp R, Hegi ME. 2008. Stem cell-related "self-renewal" signature and high epidermal growth factor receptor expression associated with resistance to concomitant chemoradiotherapy in glioblastoma. J Clin Oncol 26:3015–3024.

Mycielska ME, Fraser SP, Szatkowski M, Djamgoz MBA. 2003. Contribution of functional voltagegated Na^+ channel expression to cell behaviours involved in the metastatic cascade in rat prostate cancer: II. Secretory membrane activity. J Cell Physiol 195:461–469.

Nurse P. 2000. A long twentieth century of the cell cycle and beyond. Cell 100:71–78.

Ogawa K, Chen FF, Kuang CZ, Chen Y. 2004. Suppression of matrix metalloproteinase-9 transcription by transforming growth factorbeta is mediated by a nuclear factor-kappa B site. Biochem J 381:413–422.

Olsen ML, Schade S, Lyons SA, Amaral MD, Sontheimer H. 2003. Expression of voltage-gated chloride channels in human glioma cells. J Neurosci 23: 5572–5582.

Onganer PU, Djamgoz MBA. 2005. Small-cell lung cancer (human): Potentiation of endocytic membrane activity by voltagegated Na^+ channel expression in vitro. J Membr Biol 204:67–75.

Possani LD, Becerril B, Delepierre M, Tytgat J. 1999. Scorpion toxins specific for Na^+-channels. Eur J Biochem 264:287–300.

Prevarskaya N, Skryma R, Shuba Y. 2010. Ion channels and the hallmarks of Cancer. Trends Mol Med 16:1471–4914.

Schmidt D, Textor B, Pein OT, Licht AH, Andrecht S, Sator-Schmitt M, Fusenig NE, Angel P, Schorpp-Kistner M. 2007. Critical role for NF-κB-induced JunB in VEGF regulation and tumor angiogenesis. EMBO J 26:710–719.

Sharma GD, He J, Bazan HEP. 2003. p38 and ERK1/2 coordinate cellular migration and proliferation in epithelial wound healing. J Biol Chem 278(24): 21989–21997.

Shin I, Yakes FM, Rojo F, Shin NY, Bakin AV, Baselga J, Arteaga CL. 2002. PKB/Akt mediates cell-cycle progression by phosphorylation of $p27^{Kip1}$ at

threonine 157 and modulation of its cellular localization. Nat Med 8:1145–1152.

Song H, Moon A. 2006. Glial cell-derived neurotrophic factor (GDNF) promotes low-grade Hs683 glioma cell migration through JNK, ERK-1/2 and p38 MAPK signaling pathways. Neurosci Res 56:29–38.

Tan YH, Guo JS. 2006. Research advances in chemical component and analgesic effect of *Buthus martensii* Kirsch. Hunan Guiding J Tradit Chin Med Pharmacol 7:210–212.

Tuyt LML, Dokter WHA, Birkenkamp K, Koopmans SB, Lummen C, Kruijer W, Vellenga E. 1999. Extracellular-regulated kinase 1/2, Jun N-terminal kinase, and c-Jun are involved in NF-κB-dependent IL-6 expression in human monocytes. J Immunol 162:4893–4902.

Valster A, Tran NL, Nakada M, Berens ME, Chan AY, Symons M. 2005. Cell migration and invasion assays. Methods 37:208–215.

Vila-Carriles WH, Kovacs GG, Jovov B, Zhou ZH, Pahwa AK, Colby G, Esimai O, Gillespie GY, Mapstone TB, Markert JM, Fuller CM, Bubien JK, Benos DJ. 2006. Surface expression of ASIC2 inhibits the amiloride- sensitive current and migration of glioma cells. J Biol Chem 281:19220–19232.

Warth A, Mittelbronn M, Wolburg H. 2005. Redistribution of the water channel protein aquaporin-4 and the K^+channel protein Kir4.1 differs in low- and high-grade human brain tumors. Acta Neuropathol (Berl) 109:418–426.

Wick W, Wagner S, Kerkau S, Dichgans J, Tonn JC, Weller M. 1998. BCL-2 promotes migration and invasiveness of human glioma cells. FEBS Lett 440:419–424.

Woo MS, Jung SH, Kim SY, Hyun JW, Ko KH, Kim WK, Kim HS. 2005. Curcumin suppresses phorbol ester-induced matrix metalloproteinase-9 expression by inhibiting the PKC to MAPK signaling pathways in human astroglioma cells. Biochem Biophys Res Commun 335:1017–1025.

Zhou XH, Yang D, Zhang JH, Liu CM, Lei KJ. 1989. Purification and N-terminal partial sequence of anti-epilepsy peptide from venom of the scorpion *Buthus martensii* Karsch. Biochem J 257:509–517.